7

Modeling Surface Adsorption

7.1 Introduction

Thermodynamics, as normally defined and as presented in Chapter 3, contains no reference to surfaces. Phases, such as clay minerals and water, are assumed to exist and to equilibrate, based on their bulk properties only. However, in reality, phases interact with each other along interfaces or surfaces, the properties of which are necessarily different from the bulk properties of the phases.

On the surfaces of a phase, the normal environment of each atom is changed, and the atoms are forced to interact with atoms of a different sort, provided by the adjacent phase. In most solids and liquids, bonding is effected by electrical effects–electron transfer, electron sharing, polarization effects, and so on. In the middle of a phase there is a net charge balance, but this is disrupted at surfaces, where the three-dimensional structure is broken. Surfaces are zones where atoms are left with unsatisfied bonds, and therefore surfaces are electrically charged. These charges are accommodated somehow by the adjacent phase, and the case of most interest to geochemical modelers is the case in which one phase is a solid, and the other is water.

7.1.1 The Solid–Water Interface

This interface is quite complex, and is the subject of much active research. We present here the minimum amount of information required to understand what most geochemical modeling programs provide in the way of adsorption modeling at the present time. The capabilities present in widely used modeling programs are of two types – ion-exchange and surface complexation modeling. These represent both the historical development of the subject, and, to some extent, our understanding of two important ways in which ions adsorb to mineral surfaces.

Many minerals in aqueous solutions in the normal range of *p*H values have a negatively charged surface, which becomes neutralized by attracting positively charged particles (cations). These attracted ions may reach the solid surface and actually bond to the surface ions (inner- and outer-sphere complexes) in the *Stern layer* (Figure 7.1),

https://doi.org/10.1017/CBO9780511606274.008 Published online by Cambridge University Press

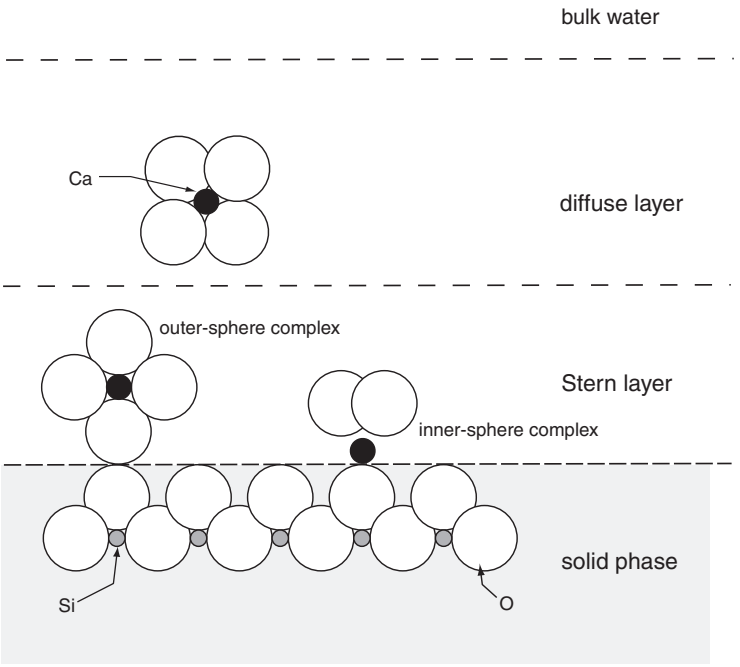

Figure 7.1. A schematic representation of a mineral surface. Hydrated aqueous ions may bond to the surface in the Stern layer, or reside close to the surface in the diffuse layer. Beyond that, "bulk water" represents water unaffected by the presence of the surface. Not to scale. (Modified from Dzombak and Hudson, 1995, Fig. 3.)

or they may simply reside close to the surface in the *diffuse layer*. The Stern layer and the diffuse layer together constitute the "electrical double layer". These two modes of adsorption can be viewed, albeit approximately, as the basis of the two kinds of adsorption modeling.

7.2 Ion-exchange

7.2.1 Cation-exchange Capacity

The negative charge on a clay mineral surface in a solution containing NaCl will be counteracted or neutralized by Na^+ ions in both the layers mentioned, but mostly in the diffuse layer. If the solution is then replaced by one containing mostly $CaCl_2$ instead of NaCl, the adsorbed Na^+ ions will be quickly replaced by (half as many) Ca^{2+} ions in a process called *ion-exchange*. More generally, whatever ions are adsorbed to the surfaces of a mineral or soil sample, they can be replaced by (exchanged for) another set of ions. This process has been more or less standardized in a batch process, in which a sample is eluted with a solution containing a standard ion, often NH_4^+, and the number of moles of ions displaced from the sample by the NH_4^+ is measured. This quantity, the

https://doi.org/10.1017/CBO9780511606274.008 Published online by Cambridge University Press

total exchangeable equivalents of cationic charge under specified conditions, is called the Cation-exchange Capacity, or CEC. It is normally measured in milliequivalents per 100 g of sample. Anion exchange can be measured in the same way, using a replacing anion, but this is usually a less important quantity.

Although "ion-exchange" is most often thought of in terms of surface as described above, it can also apply to exchange of ions from within a phase, as in the use of zeolites in water softening, or sodium for potassium exchange when K-feldspar is altered to albite at high temperatures.

7.2.2 Exchange Reactions

In the case of calcium ions replacing sodium ions, the exchange process can be written

$$Ca^{2+} + 2\,NaX = CaX_2 + 2\,Na^{+} \tag{7.1}$$

In this equation, X represents an "exchangeable site", which may actually be a site in a mineral or on a mineral surface. However, usually it is not known just how or where the ions are adsorbed, and X^- is then simply a component representing a unit charge anywhere in or close to the solid phase (Dzombak and Hudson, 1995). In either case, though, some manipulation of the CEC allows us to assign a value K_X to the ratio

$$\frac{[Na^+]^2[CaX_2]}{[Ca^{2+}][NaX]^2} = K_X \tag{7.2}$$

where [ ] denotes concentration. Using X^- as such a component, exchange equations such as (7.1) can be broken into two "half-reactions", just as redox reactions are broken into two half-cell reactions (§3.8.2). In this case, these would be

$$Na^+ + X^- = NaX \tag{7.3}$$

and

$$Ca^{2+} + 2\,X^- = CaX_2 \tag{7.4}$$

Subtracting twice Equation (7.3) from (7.4) then gives Equation (7.1). Using a suitable convention, K values can be assigned to each of these, such that K_X is obtained for the complete reaction, and it is in this "half-reaction" form that ion-exchange data is stored in databases.

There are several complications in the use of this concept.

- The measured CEC is highly sample specific, so that use of generalized ion-exchange "constants" such as K_X for conditions involving various solids is of dubious validity.
- Values of K_X are normally obtained from simple laboratory experiments involving only two cations. How to extrapolate to natural multi-component conditions is problematic.
- The concentrations of the solid phase sites (X) can be quantified, but their activities cannot, because activity coefficients are not known. Activities are therefore generally taken to be the same as the concentrations, although some rather arbitrary scheme can be used to calculate activity coefficients.

- The concentrations themselves can be calculated in different ways, depending on whether the fraction of sites occupied by an ion is given on a molar or equivalent basis (Appelo and Postma, 1993, §5.3; Dzombak and Hudson, 1995).

As pointed out by Stumm and Morgan (1996, §9.8), the "standardized" laboratory operations vary, and "it is difficult to come up with an operationally determined 'ion exchange capacity' that can readily be conceptualized unequivocally".

7.2.3 Isotherms

Ion-exchange data can also be represented in the form of isotherms, which are plots of the equilibrium concentrations of ions in the exchanger (solid) phase versus equilibrium concentrations of the same ions in the co-existing solution phase.

Distribution Coefficients and Retardation

Possibly the simplest way to describe the adsorption of an element is to define the ratio K_d as

$$K_\mathrm{d} = \frac{S_i}{C_i} \tag{7.5}$$

where S_i is the mass of adsorbed i per unit mass of solid phase and C_i is the concentration of solute i in solution. It is, in a sense, a form of Henry's Law (§3.4.1). K_d has dimensions of L^3/M, commonly ml g^{-1}. If, in a groundwater system, a solute is thus partitioned onto solid phases, its movement is retarded with respect to the groundwater flow velocity. A *retardation factor* is defined as

$$R_i = 1 + \frac{\rho_\mathrm{b}}{\theta} K_\mathrm{d} \tag{7.6}$$

where ρ_b is the bulk density of the aquifer (M/L^3) and θ is the effective porosity (dimensionless). This factor is then easily incorporated into flow equations to describe the movement of adsorbed solutes. This procedure is so commonly used, and leads to so many errors, that we have given an expanded treatment of it in §10.3.

Isotherms

Relationships such as (7.5) which describe the distribution of solutes between adsorbing surfaces and the bulk solution are of course temperature dependent, and have come to be called *isotherms*. Equation (7.5) is a particularly simple example, called a *linear isotherm* in which S is linearly proportional to C, but there are several others.

The most obvious difficulty with the distribution coefficient (7.5) is that it predicts an unlimited capacity of the surface to adsorb solutes, whereas in reality there are a finite number of sites available, and, when these are occupied by solute ions, no further adsorption will occur. We should therefore expect that a plot of adsorbed vs. bulk solution concentrations should be curved, not linear. Assuming a fixed number of

moles of identical adsorption sites (b), it can be derived that the moles of sites occupied by ion i, S_i, is

$$S_i = \frac{K_i b C_i}{1 + K_i C_i} \tag{7.7}$$

K_i is an ion-specific constant for reactions of the type

$$L + C_i = LC_i \tag{7.8}$$

where L is the concentration of a surface site arbitrarily named L, C_i is the concentration of an adsorbing ion (Ca^{2+} in the following examples), and LC_i is the concentration of sites L occupied by the adsorbing ion. In other words,

$$K_i = \frac{[LC_i]}{[L][C_i]} \tag{7.9}$$

where, as before, [ ] denotes concentration.[1] If 1 kg of water is understood, the terms can be in moles. b is thus the maximum value that LC_i can attain. A measure of site saturation is provided by θ, where

$$\theta = \frac{[LC_i]}{b} \tag{7.10}$$

which must vary from 0 to 1. Equation (7.7) is called the Langmuir isotherm. There is no difference between a Langmuir isotherm equilibrium constant and a surface complex formation constant, except that the Langmuir treatment does not explicitly involve electrostatic forces (see, e.g., Stumm and Morgan, 1996, §9.3).

Normally, isotherms are plotted as LC_i vs. C_i (see Figure 7.3a.), showing a curve asymptotic to b. Another way to plot it is *inverse* LC_i vs. *inverse* C_i. For pure Langmuir behavior, this will give a straight line with a slope of $(K_i^{-1} \cdot b^{-1})$ and an intercept of b^{-1} (see Figure 7.3b.) (Stumm and Morgan, 1996, §9.3).

Another commonly used relationship is the *Freundlich isotherm*,

$$S_i = K_F C_i^n \tag{7.11}$$

where K_F and n are constants. If $n = 1$, the above formula reduces to the linear adsorption isotherm; n is typically less than or equal to 1. It suffers from the same limitation of (7.5) in showing an unlimited capacity for adsorption, but the adjustable exponent means that it often fits experimental data quite well. It can be derived by considering surfaces to contain groups of sites, each group describable by a Langmuir isotherm.

It should also be noted that for small values of C (low aqueous concentrations), Equation (7.7) degenerates to Equation (7.5). That is, linear isotherms correspond to the low concentration region of the Langmuir isotherm.

[1] In computer programs, C_i is often an activity term, rather than a concentration. See §7.4.1.

https://doi.org/10.1017/CBO9780511606274.008 Published online by Cambridge University Press

Source	"Clean" surface	Typical surface complexes
Dzombak and Morel (1990)	$\equiv Fe^{w}OH^{\circ}$	$\equiv Fe^{w}OCu^{+}$
	$\equiv Fe^{s}OH^{\circ}$	$\equiv Fe^{s}OH_2^{+}$
Bethke (1996)	>(w)FeOH	>(w)FeOCu^{+}
(The Geochemist's Workbench™)	>(s)FeOH	>(s)FeOH$_2^{+}$
PHREEQC	Hfo_wOH	Hfo_wCu+
	Hfo_sOH	Hfo_sH2+

Table 7.1. Some ways of representing surface complexes on HFO. In programs such as The Geochemist's Workbench™ and PHREEQC, the user may define other types of notation and other surfaces. The default ones are shown.

7.2.4 Ion-exchange vs. Surface Complexation

Ion-exchange reactions and the CEC concept are used for the major ions in natural systems, rather than for minor and trace components. Although, for the most part, it is not known exactly where or how these major ions are held by the solid phases, it is probably best to envisage ion-exchange reactions as dealing with ions in the diffuse layer, rather than attached to the solid surface itself (Figure 7.1). Minor and trace element adsorption is now believed to be dominantly in the Stern layer, where they are attached to specific sites on the solid surface.

7.3 Surface Complexation

Just as exchange reactions make use of a fictive component X^{-}, so binding of elements to specific surface sites makes use of a new component for each type of site. The number of different types of sites on a mineral surface is not yet a measurable quantity, so it is, for the most part, at present, a parameter which varies between models, or between minerals within a model. For hydrous ferric oxide (HFO), for example, Dzombak and Morel (1990) concluded that two types of sites could accommodate all experimental data. These are the "strong" and "weak" sites, labelled "s" and "w" in Table 7.1.

A very useful point of view from a modeling standpoint is to consider that each type of site has a specific affinity, or a specific amount of attraction, for each type of ion in the solution, and that this can be quantitatively described by mass-action (equilibrium constant) equations. In other words, the solid sorption site behaves much like a complexing ligand in solution, and equations can be written involving sorption sites and ions, having $\Delta_r G$ values, activities and equilibrium constants. If we know the amount of surface area and the density of sites in that area, this gives the concentration ($\approx$ activity) of sorption sites. Then, if we have an equilibrium constant involving reactions between that site and various ions, we will have a system of equations that can be solved by our computer programs in the normal way to give the concentrations of surface species as well as those of the usual aqueous species.

https://doi.org/10.1017/CBO9780511606274.008 Published online by Cambridge University Press

Complexation Reactions

Consider a system consisting simply of a single solid phase in water. As discussed above, the surfaces of the solid phase will be electrically charged, even if there are no solutes in the water (Figure 7.1). However, the system as a whole is electrically neutral. This is because each charged surface induces a charge of an equal amount and an opposite sign in the adjacent solution. In other words, the solution adjacent to a negatively charged surface will have a preponderance of positively charged ions, and vice versa, the oppositely charged ones having being repelled by the surface. Whether the surface has a positive or negative charge depends largely on the solution composition and the nature of the ions adsorbed on the surface. In modeling, this charge can be calculated simply by adding up the charges on the various surface complexes.

Figure 7.2(a) shows a few of the possible arrangements. As mentioned above, the formation of each surface complex can be represented by a reaction. If the central metal ion (black circle) is Fe, the "clean" surface can be represented in various ways, depending on how we distinguish a surface complex from an aqueous complex. Some of these ways are shown in Table 7.1

The "clean" surface and the surface complex are related by reactions in the usual way, such as:

$$>(\mathrm{w})\,\mathrm{FeOH}_2^+ = >(\mathrm{w})\,\mathrm{FeOH} + \mathrm{H}^+ \qquad \log K = -7.29 \tag{7.12}$$

or

$$\equiv \mathrm{Fe^wOH}_2^+ = \equiv \mathrm{Fe^wOH}^\circ + \mathrm{H}^+ \qquad \log K = -7.29 \tag{7.13}$$

or, in PHREEQC,

$$\mathrm{Hfo\_wOH} + \mathrm{H+} = \mathrm{Hfo\_wOH2+} \qquad \log K = 7.29 \tag{7.14}$$

Note that PHREEQC writes equations in the opposite way to Dzombak and Morel (1990), a point to remember when altering databases (Appendix A).

But there is one additional factor in surface reactions, not present in aqueous phase reactions. Because the solid surface is electrically charged, it is an environment quite unlike the bulk solution, and activities and equilibrium constants must be adjusted to account for the fact that the surface sorption sites exist in a charged field.

7.3.1 The Electrical Double layer

As mentioned above, the existence of a charged surface layer induces an equal and opposite charge in the adjacent solution. This situation is described as the "electrical double layer" (EDL). The reactions controlling the charges on the surface may be modeled as described above, but the existence of the electrical field adds a complication not present in the usual aqueous reactions.

In such charged fields, chemical potentials, activities, and equilibrium constants are different from the values they would have in the absence of the charged field. By convention, equilibrium constants are given their values at the surface, before any

https://doi.org/10.1017/CBO9780511606274.008 Published online by Cambridge University Press

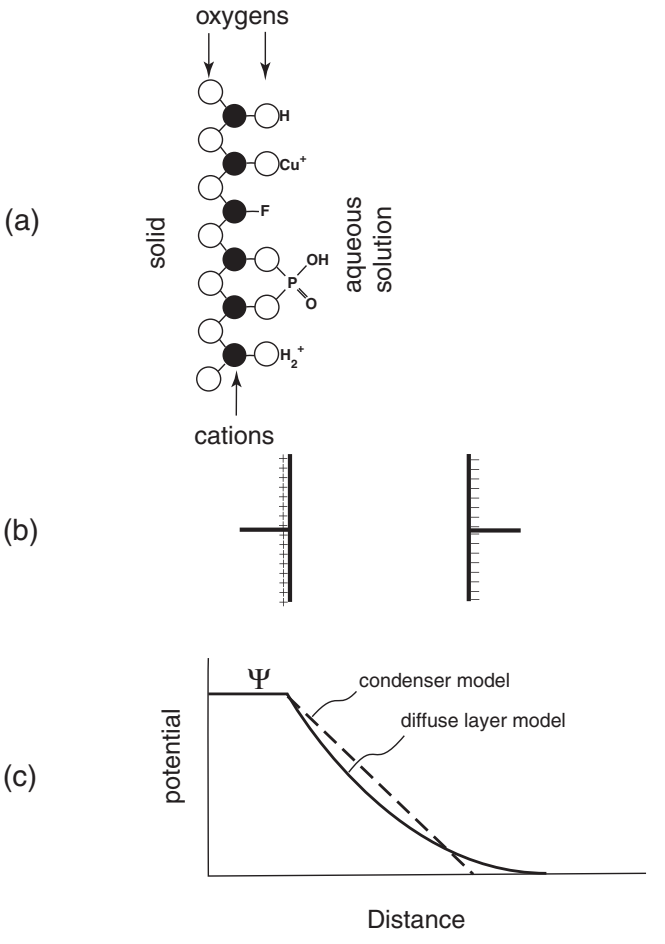

Figure 7.2. (a) Various types of surface complexes. A surface charge results from the combined positive and negative charged complexes. Adjacent to this surface in the aqueous solution, an equal and opposite charge is induced. (b) This doubly layered charge distribution can be modeled as a condenser. (c) More accurately, the potential resulting from the charged ions in the aqueous solution dies out gradually with distance from the surface, as in the diffuse layer model.

https://doi.org/10.1017/CBO9780511606274.008 Published online by Cambridge University Press

correction is applied (e.g., Equations (7.12) – (7.14)). The correction factor for the change in Gibbs energy of a mole of particles between the solution and the surface having a potential of Ψ volts is the energy (work) expended in transferring those particles from the aqueous solution to the surface. For a particle having a single electronic charge e, this work is $e \cdot \Psi$ (joules = coulombs × volts). For a mole of such charges, it is $N_a e \cdot \Psi$, where N_a is Avogadro's number. $N_a e$ is the Faraday constant, $\mathcal{F}$, so the correction term for a mole of particles having a valence (number of electron charges) of z is $z\mathcal{F}\Psi$. In other words, for a mole of charged particles (ions),

$$G_{\text{solution}} = G_{\text{surface}} + z\mathcal{F}\Psi \tag{7.15}$$

The correction factor for positive and negative ions will have opposite signs and will cancel. However, although individual surface complexation reactions (e.g., Equations (7.12) – (7.14)) are charge balanced, there is often a net change in charge of surface species (sites). For example, in Equation (7.12), $\Delta z = -1$. This is the number of charges that must be transferred from the solution to the surface, or vice versa. The $\Delta_r G^\circ$ of the surface complexation reaction will therefore have a correction factor of $\Delta z\mathcal{F}\Psi$, or

$$\Delta_r G^\circ_{\text{solution}} = \Delta_r G^\circ_{\text{surface}} + \Delta z\mathcal{F}\Psi \tag{7.16}$$

Combining this with Equation (3.26),

$$\Delta_r G^\circ = -RT \ln K$$

in which $\Delta_r G^\circ$ and K can refer to $\Delta_r G^\circ_{\text{solution}}$ and K_{solution} *or* to $\Delta_r G^\circ_{\text{surface}}$ and K_{surface}, we have

$$-RT \ln K_{\text{solution}} = -RT \ln K_{\text{surface}} + \Delta z\mathcal{F}\Psi$$

so

$$\ln K_{\text{solution}} = \ln K_{\text{surface}} - \frac{\Delta z\mathcal{F}\Psi}{RT} \tag{7.17}$$

or

$$K_{\text{solution}} = K_{\text{surface}} \cdot \exp\left(-\frac{\Delta z\mathcal{F}\Psi}{RT}\right) \tag{7.18}$$

Modeling programs deal exclusively with equilibrium constants defined for the aqueous solution, so the "intrinsic" or "surface" equilibrium constants K_{surface} obtained from the literature (e.g., Dzombak and Morel, 1990) are corrected using Equations (7.17) or (7.18).

There remains one problem – what is the value of Ψ for a charged surface?

The Gouy–Chapman Model

Although the electrical double layer (EDL) can be modeled as a simple condenser (Figure 7.2b), the distance between the plates and the dielectric constant of the material

https://doi.org/10.1017/CBO9780511606274.008 Published online by Cambridge University Press

between the plates must be known in order to relate the potential difference to the charge on the condenser. Neither of these quantities is easily determined in the present situation. The situation becomes even more difficult if the imaginary plate representing the aqueous solution is replaced by a more realistic gradual change in potential away from the surface (the diffuse layer, Figure 7.2c).

A solution to the diffuse layer problem was proposed independently by Gouy and by Chapman:

$$\sigma = (8RT\varepsilon\varepsilon_0 I \times 10^3)^{\frac{1}{2}} \sinh\left(\frac{z\Psi\mathcal{F}}{2RT}\right) \tag{7.19}$$

where σ is the surface charge density, ε is the dielectric constant of water, z is the ion charge, and ε_0 is the permittivity of free space. The original theory was developed for a single symmetrical electrolyte of concentration c. We follow Bethke (1996) in substituting the ionic strength I for c for the case of solutions with mixed electrolytes.

With known site densities, equilibrium constants for each site, and each solution component, and a way to relate surface potential to surface charge, the distribution of aqueous and surface species can now be solved in the same way as solutions with no surfaces. Bethke (1996) gives details of the method.

7.3.2 Other Surface Models

Mainly because of the work of Dzombak and Morel (1990) in providing a consistent theory and especially a self-consistent database of equilibrium constants, most widely available modeling programs use the double diffusive layer theory adopted by them. However, there are many other alternatives.

The simple condenser model or constant capacitance model has been mentioned above. It is essentially a simplified double layer theory, in which the distance between the plates can be calculated by using part of the Gouy–Chapman theory. See Stumm (1992) for details.

The triple layer model is, on the other hand, a slightly more complex version of the double layer theory, in which the surface layer is considered to be made up of two different layers – one closely bound to the surface, and one less closely bound. Several variations on this theme are to be found in the literature (Davis *et al.*, 1978).

7.4 Sorption Implementation in Computer Programs

Although there may be ambiguity in our understanding of "ion-exchange", and exactly what kinds of exchange are occurring in natural systems, there is no such ambiguity in the use of these terms in computer programs. Programs such as The Geochemist's Workbench™ and PHREEQC, which are the most versatile of presently available programs, implement these concepts in quite precise ways, which is not the same as saying that they are entirely correct, or that they will not be improved as our understanding of natural systems improves.

Programs RXN and REACT in The Geochemist's Workbench™ can account for the sorption of aqueous species onto mineral surfaces by several methods, including the two layer surface complexation model of Dzombak and Morel (1990), the constant

https://doi.org/10.1017/CBO9780511606274.008 Published online by Cambridge University Press

```
surface_data FeOH.dat
decouple Fe+++
swap Hematite for Fe+++
1 free gram Hematite
ph 5.3
2.4 mg/kg Ca++
3.5 mg/kg Mg++
0.04 mg/kg Ba++
0.4 mg/kg Na+
1.2 mg/kg Zn++
15.0 mg/kg SO4--
8 mg/kg Cl-
go
```

Table 7.2. A REACT script to calculate the amounts of various ions adsorbed by 1 g of HFO. From The Geochemist's Workbench™ User's Guide.

capacitance and constant potential models, ion-exchange, distribution coefficients (K_d), and Langmuir isotherms. Program PHREEQC also includes the Dzombak and Morel formulation and data, and ion-exchange reactions (and data). Distribution coefficients and Langmuir isotherms are not explicitly included, but can be simulated nonetheless.

7.4.1 Examples

To show how these programs work, we consider a couple of examples from The Geochemist's Workbench™ User's Guide, then repeat them with PHREEQC. Examples of more complex systems are considered in later chapters.

The Dzombak and Morel Model for Adsorption on HFO

The Geochemist's Workbench™ Consider a dilute solution containing several ions in contact with the adsorbing surfaces of hydrous ferric oxide (HFO). A script for program REACT is shown in Table 7.2.

The Geochemist's Workbench™ stores the Dzombak and Morel data in a file called `FeOH.dat`. The program calculates the sorbing surface area and available sites from the mass of mineral (1 g) and data in `FeOH.dat`.

PHREEQC A script to perform the same calculation in PHREEQC is shown in Table 7.3. The Dzombak and Morel data are included in the default PHREEQC database. In Table 7.3, the key word `SURFACE` defines the surface properties to be the same as those in the REACT example, and `EQUILIBRIUM_PHASES` declares that hematite is in equilibrium

https://doi.org/10.1017/CBO9780511606274.008 Published online by Cambridge University Press

```
TITLE Example from GWB User's Guide
SURFACE 1
        -equilibrate with solution 1
        Hfo_sOH        6.262e-5    600.    1.0
        Hfo_wOH        2.505e-3
EQUILIBRIUM_PHASES 1
    Hematite    0.  0.006262
SOLUTION 1
     -units mg/kgw
     ph     5.3
     Ca     2.4
     Mg     3.5
     Ba     .04
     Na     0.4
     Zn     1.2
     S(6)     15.
     Cl      8     charge
SELECTED_OUTPUT
     -file  sel_HFO.out
     -reset false
USER_PUNCH
     -headings  Ba  Ca SO4  Zn
     -start
     10 sorbed_Ba = mol("Hfo_sOHBa+2")  + mol("Hfo_wOBa+")
     20 sorbed_Ca = mol("Hfo_sOHCa+2")  + mol("Hfo_wOCa+")
     30 sorbed_SO4= mol("Hfo_wOHSO4-2") + mol("Hfo_wSO4-")
     40 sorbed_Zn = mol("Hfo_sOZn+")    + mol("Hfo_wOZn+")
     50 frac_Ba   = sorbed_Ba/ (sorbed_Ba + TOT("Ba"))
     60 frac_Ca   = sorbed_Ca/ (sorbed_Ca + TOT("Ca"))
     70 frac_SO4  = sorbed_SO4/(sorbed_SO4 + TOT("S(6)"))
     80 frac_Zn   = sorbed_Zn/ (sorbed_Zn + TOT("Zn"))
     90 PUNCH frac_Ba  frac_Ca  frac_SO4  frac_Zn
     -end
END
```

Table 7.3. A PHREEQC script to calculate the amounts of various ions adsorbed by 1 g of HFO.

https://doi.org/10.1017/CBO9780511606274.008 Published online by Cambridge University Press

	Fraction sorbed	
	REACT	PHREEQC
Ba	0.003028	0.003036
Ca	0.0009716	0.0009721
SO4	0.8477	0.8477
Zn	0.4018	0.4022

Table 7.4. Comparison of sorption results from REACT and PHREEQC.

with the solution (SI = 0.0). The `USER_PUNCH` keyword is useful here, because we want results in the same form that REACT provides, which is the fraction of element sorbed, where the total amount of the element is the amount sorbed *plus* the original solution molality. Note that, unless instructed otherwise, both programs calculate the amount sorbed in equilibrium with the solution composition given, so the total amount of element after sorption can be quite a bit greater than in the original solution. `USER_PUNCH` allows us to print out a file with this information.

The results from the two programs are shown in Table 7.4.

The Langmuir Isotherm

The Geochemist's Workbench™ Program REACT calculates the amount of elements adsorbed according to the Langmuir isotherm by first reading a user prepared file which gives the adsorption reactions and their equilibrium constants. The format of this file is given in The Geochemist's Workbench™ distribution in an example file to use as a template. In this file, both Ca and Sr are given reactions and constants for a single adsorption site called L. In our example, we have used this file, but eliminated the Sr adsorption, so that only Ca adsorbs on the site L, according to the reaction

$$L + \mathrm{Ca} = L\mathrm{Ca} \qquad \log K = 2.1 \tag{7.20}$$

where L is the concentration of surface sites, Ca is the *activity* of the calcium ion, and LCa is the adsorbed concentration of calcium.

The exchange capacity (the total number of sites, and therefore the maximum amount of adsorbed Ca) in moles (0.01) is given in the input script. The script shown in Table 7.5 is taken from the User's Guide, substituting our new file name for the modified surface data. Because we want to use a number of different Ca concentrations, we must modify the script and run it repeatedly.

PHREEQC Program PHREEQC does not contain an explicit provision for calculating Langmuir isotherms, but has enough options in the `SURFACE` data block to do the same thing. A script to perform the same calculation done by REACT is shown in Table 7.6.

In this script, the data blocks `SURFACE_MASTER_SPECIES` and `SURFACE_SPECIES` perform the same function as the separate file we prepared for REACT, `langmuir2.dat`. They define a surface site L, and give the equilibrium constant for the adsorption reaction. The `SURFACE` data block equilibrates the solution

https://doi.org/10.1017/CBO9780511606274.008 Published online by Cambridge University Press

```
surface_data = Langmuir2.dat
pH = 8.3
Cl-   = 19000 mg/kg
Ca++  =   400 mg/kg
Sr++  =    10 mg/kg
Mg++  =  1300 mg/kg
Na+   = 10700 mg/kg
K+    =   400 mg/kg
SO4-- =  2700 mg/kg
exchange_cap = 0.01 moles
go
```

Table 7.5. A REACT script to calculate adsorption of Ca according to the Langmuir isotherm.

```
TITLE Langmuir isotherm (from GWB) SURFACE_MASTER_SPECIES
        L        L
SURFACE_SPECIES
        L = L
          log_k    0.0
        L + Ca+2 = LCa+2
          log_k    2.1
SURFACE 1
        -equilibrate with solution 1
        -no_edl
        L   0.01
SOLUTION 1
        -units mg/kgw
        ph        8.3
        Ca        10000
        Mg        1300
        Na        10700
        Sr        10
        K         400
        S(6)      2700
        Cl        19000        charge
END
```

Table 7.6. A PHREEQC script to calculate Ca adsorption according to a Langmuir isotherm.

https://doi.org/10.1017/CBO9780511606274.008 Published online by Cambridge University Press

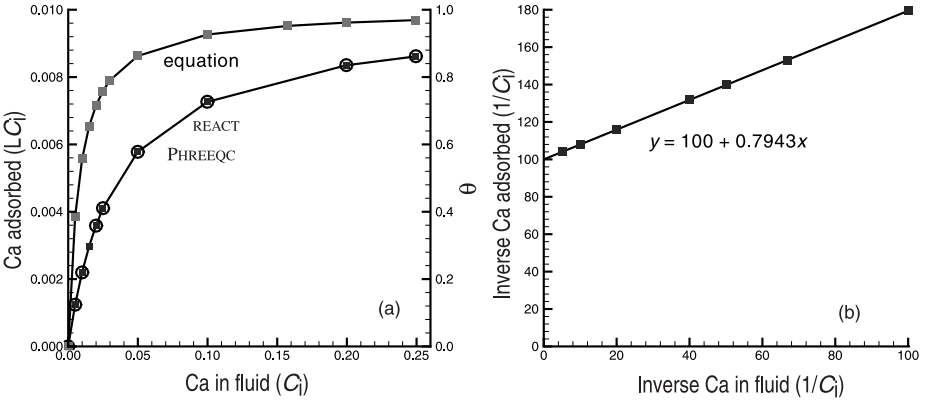

Figure 7.3. (a) Comparison of the Langmuir isotherm calculated by REACT, PHREEQC, and Equation (7.7). (b) Inverse plot and least squares fit for the equation results.

(SOLUTION 1) with this surface and contains the instruction -no_edl, which turns off all electrostatic calculations, those necessary for the electrostatic double layer theory. It also defines the total number of L sites. There is no explicit mention of Langmuir isotherm because, as mentioned above, there is no difference between a Langmuir isotherm equilibrium constant and a single-site surface complex formation constant, which PHREEQC understands.

This script must be run several times, varying the Ca content to define the complete isotherm. Alternatively, the script can be extended, with each calculation separated by an END statement. Using the script shown in Table 7.6, the program prints a voluminous output file which contains a lot of data besides the adsorption data. We could add the following statements to make the task of finding these data easier.

```
SELECTED_OUTPUT
        -file   lang.sel
        -reset  false
USER_PUNCH
        -headings  Total_Ca  Ca+2  Adsorbed_Ca
        -start
        10 PUNCH TOT("Ca")  MOL("Ca+2") MOL("LCa+2")
        -end
```

These cause another output file to be written, lang.sel, containing only the total Ca, the Ca^{2+} molality, and the moles of adsorbed Ca.

The calculated isotherms from REACT and from PHREEQC are virtually identical, as shown in Figure 7.3(a). Note that although the two programs give the same results, these are quite different from those obtained from Equation (7.7) with the same data ($K_i = 10^{2.1}$; $b = 0.01$; $C_i = 0 \rightarrow 0.25$), although all results tend towards a maximum of 0.01, or $\theta = 1$, as they should. This is because both programs use the *activity* of Ca^{2+} in their calculations, rather than the nominal concentration. The activity coefficient of Ca^{2+} is about 0.2 under these conditions, which accounts for the results from the two

https://doi.org/10.1017/CBO9780511606274.008 Published online by Cambridge University Press

programs being a factor of about 0.2 less than the results from the equation (see §3.4.1 for the activity–concentration relationship).

The expected results for the inverse plot (Figure 7.3b) are

$$\text{intercept} = b^{-1} = 1/0.01 = 100, \text{ and}$$

$$\text{slope} = K^{-1} \cdot b^{-1} = (1/10^{2.1}) \cdot 100 = 0.7943.$$

The inverse plot gives the expected results for the equation results. An inverse plot of the computer program results gives a straight line, but with a different slope and intercept.

7.4.2 Why Surface Modeling is Not Perfect

Dzombak and Morel (1990) performed a great service for surface modelers in systematizing a huge body of diverse literature on hydrous ferric oxide (HFO) research, and presenting it in a form which readily lent itself to use by programmers. In doing so, they made a number of decisions about HFO, such as the surface area, number of active sites, site densities, and so on (Table 7.7), as well as of the type of model and the data to use. All these choices find their way into the default values of these parameters of the programs written subsequently. There is nothing intrinsically wrong with these choices; they may well be the best possible overall values. However, they cannot be the best values for all possible applications.

For one thing, hydrous ferric oxide, although a very important adsorber in natural systems, is an extremely complex substance, having a wide range of physical properties (see Cornell and Schwertmann (1996) for a recent summary). Therefore, it is never certain that the default properties of HFO or the experimental data on HFO chosen by Dzombak and Morel (1990) will be appropriate for given natural systems. Also, the amount of this phase present is often poorly known.

It must also be remembered that HFO is only one of the many phases in natural samples, and although an important adsorber, it is not the only one. However, it is the only one in most models. Possibly, other phases, although weak adsorbers, could play important roles by being present in large amounts.

Furthermore, most experimental work applies to simple laboratory systems, and a great deal more work will be needed to understand adsorption quantitatively in complex natural systems. Particularly lacking is a mechanistic understanding of the role of the solid phase, and any ability to predict surface complexation constants. A promising start in this direction is provided by Sverjensky (1993, 1994), and Sverjensky and Sahai (1996).

7.5 Retardation of Radionuclides at Oak Ridge

Saunders and Toran (1995) used the diffusive double layer model of Dzombak and Morel (1990) to model the role of HFO in retarding radionuclide migration at the Oak Ridge Reservation, Tennessee. Large amounts of low-level radioactive wastes were disposed into shallow, unlined lagoons and trenches, resulting in concerns for their potential migration. Saunders and Toran (1995) used MINTEQA2 to perform speciation, solubility,

Site density:		
strong	5.62×10^{-5} mol g^{-1}	5×10^{-3} mol mol^{-1}
weak	2.25×10^{-3} mol g^{-1}	0.2 mol mol^{-1}
Surface area	600 m^2 g^{-1}	600 m^2 g^{-1}
Molecular formula weight	89 g mol^{-1}	89 g mol^{-1}

Table 7.7. Surface properties of hydrous ferric iron oxides. Data from Dzombak and Morel (1990).

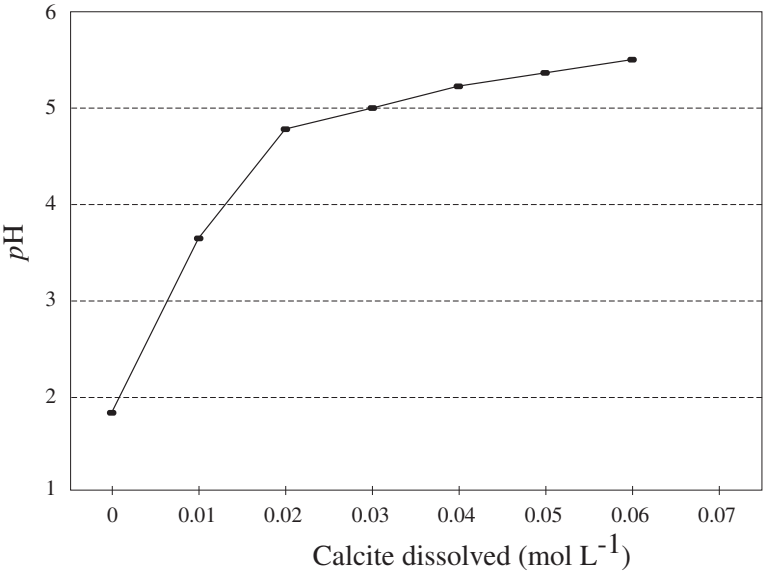

Figure 7.4. Results of MINTEQA2 calcultions in Saunders and Toran (1995).

and surface complexation calculations and compared the modeling results with field data. In one of their modeling applications, the acidic water from S-3 pond, Y-122 was allowed to dissolve calcite – a reaction assumed to be the dominant neutralization mechanism in the aquifer. Aqueous speciation, Saturation Indices of minerals, and surface complexation were calculated at each *p*H increment. Apparently, supersaturated solids were not allowed to precipitate in their model runs. An average amount of amorphous HFO of 0.9 wt.% was used for calculating the sorbent concentrations, and the surface properties recommended by Dzombak and Morel (1990) were used for their amorphous iron oxide (Table 7.7). The intrinsic complexation constants of Dzombak and Morel (1990) were added to the MINTEQA2 surface complexation reaction database.

The modeling results are shown in Figures 7.4 and 7.5. MINTEQA2 calculations show possible solubility control of Fe and Cd by precipitation of siderite ($FeCO_3$) and otavite ($CdCO_3$), and significant retardation of heavy and transition metals by HFO in the order of Pb > Zn > Ni > ^{60}Co. The model also predicts little sorption of ^{90}Sr by Fe oxyhydroxide at *p*H < 7. The modeling results illustrate the *p*H-dependent nature

https://doi.org/10.1017/CBO9780511606274.008 Published online by Cambridge University Press

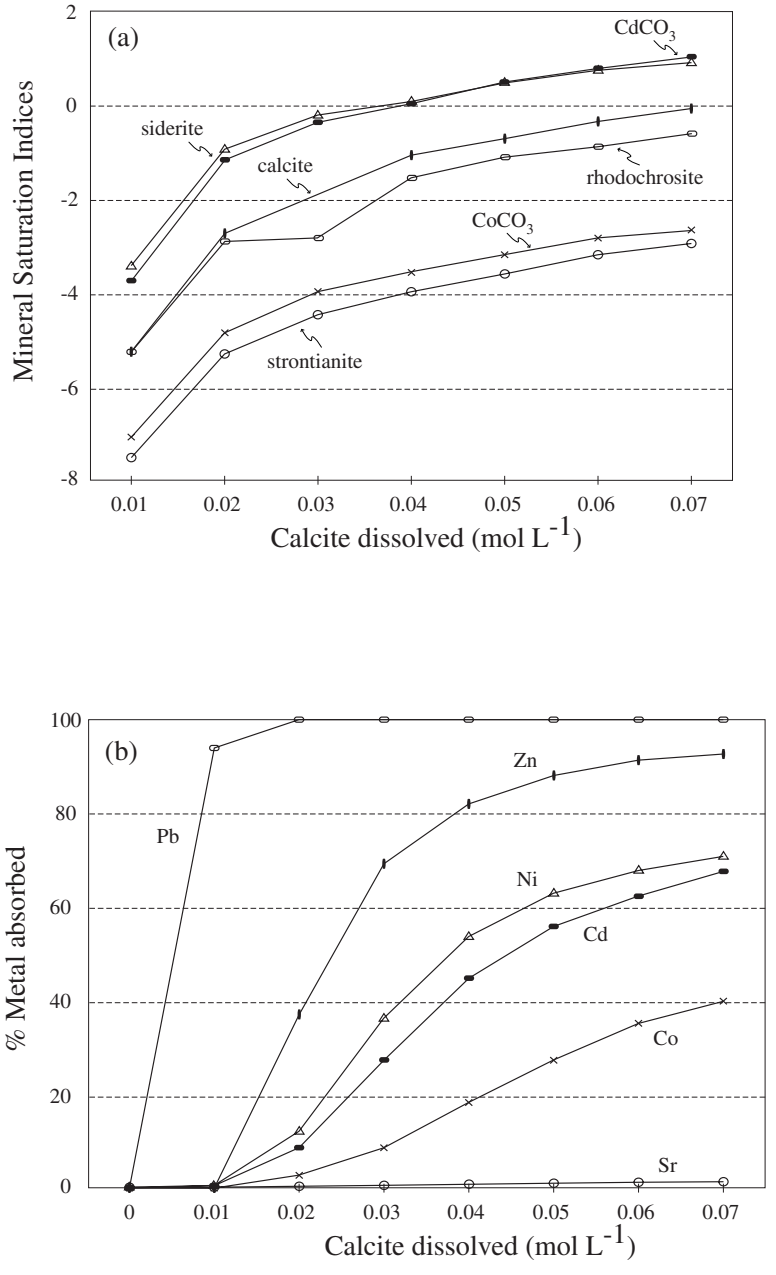

Figure 7.5. Saturation Indices (a) and surface adsorption (b) calculated from MINTEQA2 in Saunders and Toran (1995).

https://doi.org/10.1017/CBO9780511606274.008 Published online by Cambridge University Press

Calculation of Sorbent Concentrations: Example 1

Saunders and Toran (1995) used an average of 0.9 wt.% amorphous $Fe(OH)_3$ in soil around the Oak Ridge burial ground for calculating sorbent concentrations. The amorphous iron concentrations were obtained from the sequential extraction techniques. To calculate the surface sites in their surface complexation modeling, they used a soil porosity of 40% and dry density of 2.5 g cm^{-3}, respectively. The calculation is recapped here:

For a volume of 1000 cm^3 aquifer, the solid matrix portion has a volume of

$$1000\,cm^3 \times (1 - 40\%) = 600\,cm^3$$

The weight is

$$600\,cm^3 \times 2.5\,g\,cm^{-3} = 1500\,g$$

The total $Fe(OH)_3$ in the soil matrix is

$$1500\,g \times 0.9\% = 13.5\,g$$

The volume of pore water in a 1000 cm^3 aquifer is 400 cm^3. The amount of $Fe(OH)_3$ in contact with 1.0 liter of water is

$$13.5\,g/0.40 = 33.75\,g\,L^{-1} \text{ as } Fe(OH)_3$$

With a formula weight of 89 g,

$$\text{the sorbent concentration} = 33.75/89 = 0.34\,mol\,L^{-1}$$

of metal sorption onto HFO. Comparison with field monitoring data shows that the model-predicted relative mobilities are basically consistent with field data. It should be noted that a number of assumptions are made for the modeling runs. For example, Saunders and Toran (1995) discussed the omission of the possible sorption of metals to precipitating Fe and Al oxyhydroxides.

7.6 Mobility of Radionuclides at a Uranium Mill Tailings Impoundment

In the discussion of the Bear Creek Uranium site in §6.2, we note that more than a dozen regulated metals and radionuclides have elevated concentrations in the acidic plume. The relative mobility of the radionuclides at the leading edge of the plume can be estimated by using the diffusive double layer model of Dzombak and Morel (1990).

https://doi.org/10.1017/CBO9780511606274.008 Published online by Cambridge University Press

Calculation of Sorbent Concentrations: Example 2

Parkhurst (1995, example 10) also did calculations of sorbent concentrations in his surface complexation modeling for the central Oklahoma aquifer. The amount of extractable iron in sediments is from 1.6 to 4.4%. Porosity is 22%, and rock density is 2.7 $g\,cm^{-3}$. For a 2 wt.% iron, the solid concentrations should be calculated as follows. The total weight for a volume of 1000 cm^3 aquifer is

$$1000\,cm^3 \times (1 - 22\%) \times 2.7\,g\,cm^{-3} = 2106\,g$$

The total iron in the solid is

$$2106\,g \times 2\% = 42.12\,g$$

The amount of iron in contact with 1.0 liter of pore water is

$$\text{solid concentration} = 42.12\,g/0.22L = 192\,g\,L^{-1} \text{ as Fe}$$

or

$$\text{solid concentration} = 306\,g\,L^{-1} = 3.4\,mol\,L^{-1} \text{ as } Fe(OH)_3$$

Parkhurst (1995) assumed 10% extractable iron is in amorphous form so that the sorbent concentrations he used is 0.38 $mol\,L^{-1}$.

7.6.1 Why Geochemical Modeling?

At the Bear Creek Uranium site, groundwater monitoring data have been collected on a quarterly basis. These data outline the distribution of the hazardous constituents over the time and provide an observational basis on the mobility of the radionuclides under the site's geologic conditions. Geochemical modeling can provide interpretations of the observational data so that prediction of potential migration in the future can be built on a scientific basis. For hazardous constituents that show no or limited mobility at the site, geochemical modeling can provide a plausible interpretation, and, hence, strengthen the case for eliminating them in further considerations. For hazardous constituents that show migration at the site, quantitative predictions of their concentrations in the future have to be provided to the decision makers.

7.6.2 Modeling Approach

As discussed in §6.2, the migrating acid plume has a *p*H of about 4.5, buffered by the precipitation of amorphous $Al(OH)_3$, and carries with it the elevated concentrations of radionuclides and hazardous constituents. When the acidic water encounters calcite in the aquifer in the downgradient area, calcite dissolution occurs, and that buffers the

https://doi.org/10.1017/CBO9780511606274.008 Published online by Cambridge University Press

Al	3.79×10^{-7}	Mg	4.19×10^{-2}
Ba	1.48×10^{-7}	Mn	1.27×10^{-3}
C	5.0×10^{-2}	Na	1.27×10^{-2}
Ca	6.73×10^{-3}	SO4	3.27×10^{-2}
Cl	1.15×10^{-2}	Si	3.62×10^{-4}
F	1.07×10^{-5}	Gypsum	0.082
Fe	1.6×10^{-8}	$Al(OH)_3$	0.013
K	1.82×10^{-3}	$Fe(OH)_3$	0.038
*p*H	6.6		

Table 7.8. Composition of MW-77 in mol L^{-1} after being neutralized by 0.08 mole calcite.

groundwater *p*H to about 6.5.

Therefore, we take two steps in modeling. First, the acidic water is neutralized by titrating of calcite. The amounts of Fe and Al hydroxides precipitated from this titration are then used in the subsequent speciation and complexation modeling.

In the first step, acidic water of about *p*H 4.5 was first neutralized to a *p*H of 6.6 by titrating calcite using PHREEQC (see §8.3). Neutralization of the acid water caused the precipitation of gypsum, and Al and Fe hydroxides. This kind of reaction path modeling will be discussed in Chapter 8. Here, we only present the resulting compositions of the neutralized water and precipitated solids in Table 7.8.

In the second step of the modeling exercise, speciation and surface adsorption in the neutralized water were modeled using the geochemical code MINTEQA2. Analytical concentrations of Cd, Ni, Be, and U (5.5, 65, 4.1, and 22 $\times 10^{-6}$ mol L^{-1}, respectively) were used as input concentrations. The surface properties and surface complexation constants were taken from Dzombak and Morel (1990). Due to the lack of experimental data for Al hydroxides, we assume that all Al hydroxides have the same sorptive properties as Fe hydroxide and that the mass of Al hydroxide was added to the Fe hydroxide concentrations. The total sorbent concentration is 5.3 g/L as $Fe(OH)_3$, which is calculated from the first step. MINTEQA2 was used to calculate the partitioning of these ions between the aqueous phase and ferric iron hydrous oxide (HFO) surfaces.

7.6.3 Modeling Results

Tables 7.9 and 7.10 show the results from MINTEQA2. The model predicts that the dominant aqueous species for uranium and nickel in water are carbonate complexes. A significant proportion of sorption sites on the ferric oxides are occupied by sulfate ions, which results in fewer sorption sites available for metals and radionuclides.

7.6.4 Comparison with Field Data

Comparing the modeling results with site monitoring data shows that the predicted sequence of the contaminant mobility, Be < Cd < Ni < U, is consistent with the metal distribution at the site. Surface complexation has essentially immobilized Be and Cd

https://doi.org/10.1017/CBO9780511606274.008 Published online by Cambridge University Press

Component	Species	Distribution (%)[a]
Be^{2+}	Be^{2+}	100 [b]
Ni^{2+}	$NiCO_3(aq)$	88
	$NiHCO_3^+$	12
Cd^{2+}	Cd^{2+}	100
UO_2^{2+}	$UO_2(CO_3)_2^{-2}$	76
	$UO_2(CO_3)_3^{-4}$	24
Sorption site 1	$\equiv SO1HCa^{2+}$	45
	$\equiv SO1HSO_4^{-2}$	17.3
	$\equiv SOH1^\circ$	13
	$\equiv SO1H2^+$	11
	$\equiv S1SO_4^-$	7
	$\equiv SO1Ni^+$	3
	$\equiv SO1Be^+$	2
Sorption site 2	$\equiv SO2HSO_4^{-2}$	34
	$\equiv SOH_2^\circ$	26
	$\equiv SO2H_2{}^+$	22
	$\equiv S2SO_4^-$	15
	$\equiv SO2UO_2^+$	2

Table 7.9. Species distribution in the aqueous phase and on sorption sites, as calculated by MINTEQA2.

[a] Aqueous speciation is normalized to aqueous phase only.
[b] No other aqueous Be species available in the database.

(100% and 98% sorbed onto the surfaces, respectively) . Surface adsorption onto HFO that amounts to precipitation from one pore volume of fluid can control Be and Cd to <0.01 mg L^{-1}, the groundwater protection standard. The observational data show that Be is not seen outside of the acid plume, and Cd has limited migration outside of the plume. Modeling results show that 87% Ni is sorbed onto Fe oxyhydroxide at the time of neutralization, but significant concentrations remain in the aqueous phase. This is consistent with the monitoring data that show significant transport of nickel. The modeled equilibrium concentration of 4.8 mg L^{-1} is close to the measured concentrations at the edge of the current acid plume.

However, the predicted uranium concentration at the edge of the plume is far higher than the observation. Observational data indicate that the maximum uranium concentration outside of the plume is less than 92 pCi/L, while the model predicts it to be in excess of 1000 pCi/L. This discrepancy between observed and predicted uranium concentrations is an indication that the model parameters used to predict U partitioning may not accurately represent conditions at the site. Examination of Dzombak and Morel's (1990) work reveals that they have used a predicted surface complexation constant rather than retrieve a value from experiments. Newer experimental data show that uranium(VI) adsorption onto ferrihydrite can be fitted by a two-site model with a bidentate complex (Waite *et al.*, 1994). However, this type of modeling ability is not included with MINTEQA2. Another explanation could be that co-precipitation is ignored, but apparently is a major attenuation mechanism at a similar site (Opitz *et al.* 1983).

https://doi.org/10.1017/CBO9780511606274.008 Published online by Cambridge University Press

Species	Dissolved ($mol\,kg^{-1}$)	(%)	Sorbed ($mol\,kg^{-1}$)	(%)
UO_2^{2+}	2.067×10^{-5}	94	1.325×10^{-6}	6
Al^{3+}	3.800×10^{-7}	100	0.000×10^{-1}	0
Ba^{2+}	8.083×10^{-8}	53.9	6.917×10^{-8}	46.1
CO_3^{2-}	5.000×10^{-2}	100	0.000×10^{-1}	0
Ca^{2+}	5.671×10^{-3}	84.6	1.029×10^{-3}	15.4
Cl^-	1.140×10^{-2}	100	0.000×10^{-1}	0
F^-	1.00×10^{-5}	100	0.000×10^{-1}	0
Fe^{3+}	1.600×10^{-8}	100	0.000×10^{-1}	0
K^+	1.820×10^{-3}	100	0.000×10^{-1}	0
Mg^{2+}	4.180×10^{-2}	100	0.000×10^{-1}	0
Mn^{2+}	1.270×10^{-3}	100	0.000×10^{-1}	0
Na^+	1.260×10^{-2}	100	0.000×10^{-1}	0
PO_4^{3-}	2.316×10^{-10}	0.2	9.977×10^{-8}	99.8
SO_4^{2-}	3.212×10^{-2}	98.2	5.838×10^{-4}	1.8
H_4SiO_4	3.620×10^{-4}	100	0.000×10^{-1}	0
Be^{2+}	7.703×10^{-9}	0	4.099×10^{-5}	100
Cd^{2+}	1.094×10^{-7}	2	5.391×10^{-6}	98
Ni^{2+}	8.240×10^{-6}	12.7	5.676×10^{-5}	87.3
H_2O	1.318×10^{-6}	-0.3	-4.862×10^{-4}	100.3
E^-	0.000×10^{-1}	0	0.000×10^{-1}	0
H^+	6.327×10^{-2}	99.5	3.308×10^{-4}	0.5

Table 7.10. Results of MINTEQA2 calculations of adsorption onto hydrous ferric iron oxide (HFO).

7.6.5 Discussion of Modeling Results

Are the modeling results practically useful? In this case, they are. Surface complexation and speciation modeling is shown to be an effective screening tool for evaluating the mobility of metals and radionuclides at the site. This screening resulted in an explanation for the mechanism of natural attenuation for hazardous constituents that are judged to be immobile from observation data. Elimination of these constituents from further analysis, e.g., solute transport modeling, can result in cost savings.

However, as we noted early in this chapter, numerous assumptions are employed in the field applications of surface complexation models. Davis *et al.* (1998) noted that surface complexation models are mainly developed from well-controlled laboratory experiments. It is unclear how the models can be applied to soil and sediments where the double layers of the heterogenous particles may interact and the competitive adsorption of many different ions can cause significant changes in the electrical properties of mineral–water interfaces.

7.7 Adsorption of Arsenic in Smelter Flue Dust

Doyle *et al.* (1994) used the triple layer model of Davis *et al.* (1978) to model surface adsorption of arsenic onto amorphous ferric oxides. Copper smelting has produced

https://doi.org/10.1017/CBO9780511606274.008 Published online by Cambridge University Press

Surface area	200 $m^2\ g^{-1}$
Site density	11.4 site nm^{-2}
Inner layer capacitance	1.4 $F\,m^{-2}$
Outer layer capacitance	0.2 $F\,m^{-2}$

Table 7.11. Surface properties for the triple layer model for amorphous Fe oxide from Davis *et al.* (1978).

metal bearing flue dust as a by-product of smelter exhaust streams. This flue dust contains high concentrations of hazardous metals such as arsenic (16 500–79 200 ppm), zinc (19 200–49 000 ppm), lead (9 260–32 300 ppm), copper (69 400–244 000 ppm), etc. Safe disposal of these wastes into the environment is a concern. To evaluate disposal practices, Doyle *et al.* (1994) conducted column experiments. Flue dust waste cake from the Cashman hydrometallurgical processes was packed into glass columns and the columns leached with de-ionized water. Two types of flue dust were used to fill the columns: one from a batch reactor and one from a continuous reactor. The waste cakes were analyzed for their mineralogical compositions using an electron microprobe, and leachate was collected for analysis.

The authors first used MINTEQA2 to evaluate the solubility control of As concentrations in the effluents of column experiments. They found that it was necessary to replace the $\log K$ values for the arsenic aqueous species and the mineral scorodite [$FeAsO_4 \cdot 2H_2O$] in the MINTEQA2 database with those for the Fe–As–SO_4 systems from Robins (1990) in order to match the simulation and experimental results. From the microprobe study they found 1 μm-sized, As-bearing phases having a stoichiometric composition close to scorodite.

Sorption of $HAsO_4^{2-}$, $H_2AsO_4^-$ and SO_4^{2-} was simulated using MINTEQA2. The sorption of cations was not simulated. Surface properties and surface complexation constants were taken from Davis and Leckie (1978, 1980) and Davis *et al.* (1978) (Table 7.11). Varying the surface parameters over the ranges given in the original papers did not substantially change the modeling results. The sorbent concentration is assumed to be 1% of the total Fe in the flue dust present as $Fe(OH)_3$. The authors claim that variation of the sorbent concentrations up to two orders of magnitudes did not change the simulated results (mostly solubility control, not surface adsorption; see below).

The authors found that the model-predicted As concentration is close to the leachate concentrations from the column packed with dust from the continuous reactor (1 120 $\mu g\,L^{-1}$ versus 1 330 $\mu g\,L^{-1}$), when the solubility product of scorodite from Robins (1990) and the triple layer model is used. Only 11% As in the system was sorbed onto hydrous ferric oxide surfaces. Arsenic concentrations in the leachate are largely controlled by scorodite solubility. It should also be pointed out that simulations using solubility only and without including surface adsorption resulted in a closer match (1 270 $\mu g\,L^{-1}$ versus 1 330 $\mu g\,L^{-1}$). For the simulation of the column experiments using wastes from the batch-reactor, the triple layer model predicted too low an As concentration (33 $\mu g\,L^{-1}$ versus 120 $\mu g\,L^{-1}$).